Summer Internship Project
Report

Nanoparticle synthesis using microfluidics

Submitted by

KALING VIKRAM SINGH
Roll no : 2011074
School of physical sciences, NISER

Under the guidance of

Dr Vida A Dennis
Center for NanoBiotechnology Research (CNBR)

Department of Life Sciences
Alabama State University
Montgomery

Summer Internship 2023

Acknowledgment

The successful accomplishment of this report is the outcome of the contribution of a number of people to whom I am grateful and thank them from the very deep of my heart. In the beginning I would like to convey my sincere gratitude to my professor and advisor Dr Vida A Dennis, Department of life sciences, Alabama state university. Without her guidance and assistance, this report would not have seen the light of day.

I would like to thank Dr Rajnish Sahu who guided me throughout the tenure and helped me in conducting experiments and tests. I would also like to thank NISER and Alabama state university for providing me an opportunity for arranging the internship to broaden my exposure to sciences and industries.

Abstract

Microfluidics, a new subject at the intersection of science and technology, has revolutionized fluid manipulation by utilizing the potential of miniaturized devices with intricate micro-scale channels and chambers. This cutting-edge discipline holds enormous promise and has cleared the way for ground-breaking advances in a wide range of scientific and industrial applications. One of its primary characteristics is its capacity to accurately control fluid behavior, which opens the door to a multitude of possibilities such as reactions, separations, and the detection of various chemicals with unrivaled precision and efficiency. The success of the study was dependent on the thorough optimization of various critical aspects, each of which contributed to the creation of nanoparticles encapsulating Bovine Serum Albumin (BSA). Parameters such as the flow rate ratio (FRR), total flow rate (TFR), and polymer content were carefully standardized to assure reproducibility and dependability. These factors play a critical role in defining the size, shape, and encapsulation effectiveness of the resultant nanoparticles. This research highlights the various parameters for standardization of microfluidics in nanoparticle manufacturing and encapsulation, paving the path for novel applications in biomedicine and materials engineering.

Contents

Chapter 1

Introduction

1.1 Mixing mechanics

Microfluidics is the science and technology of fluid dynamics at micro or nanoscales. This includes the study of the micro-mixing of two or more fluids, the design of equipment to achieve better mixing, the study of flow parameters, etc in small channels/tubes having dimensions typically, between 10 to 100 micrometers. Microfluidics is essentially used for many drug-related tests and synthesis of nanoparticles transport drugs in blood. The use of microfluidics started extensively in the 1980s when they were used in DNA chips and ink-jet printheads, although there was no major use until 2006 when Fluigents started using microfluidics pumps for various industrial applications. Later, its use in drug-related studies and research grew due to various qualities of the technique. The use of microfluidics in medicine is essentially due to its reproducibility and robustness in various conditions [1].

The physics behind microfluidics is very interesting and extensively studied at higher levels due to its industrial applications. The study of microfluidics is special due to its high surface area-to-volume ratio which results in the domination of surface factors over volumetric factors [2]. This means that viscosity and density are more important compared to volumetric factors such as inertia. Due to the high surface area-to-volume ratio, resulting in rapid heat and mass transfer rates, microfluidics is a suitable candidate for equipment like micro-heat exchangers, microreactors, etc.

The fluids have two basic bulk properties, viz density, and viscosity. Viscosity is a measure of relative friction between two liquid interfaces. Higher viscosity leads to lower fluid mixing as any force that is responsible for mixing dies out before the whole process is complete. The density (ρ) is another property that plays an important role in mass transfer phenomena and thus, affects the flows. The fluids are considered incompressible, leading to constant net density (ρ) as a function of space and time. In a mixture of two or more fluids, less dense fluid is pushed

away from the channel walls while a denser fluid is partially absorbed by it. This effect becomes more pronounced as the fluid density ratio rises, which increases the area of the miscible fluids' interface and, as a result, improves the mixing efficiency in this regime. Thus, a higher density ratio leads to better mixing of the liquids [3].

Aref [4] defines "mixing" as a physical process where both stirring and advection occurs simultaneously. Stirring is the pure advective mixing of material blobs without any diffusive action. Thus, mixing can be said to occur in two phases: 1: Stirring and 2: Diffusion.

Diffusion is the movement of particles from an area of higher concentration to an area of lower concentration due to random motions. This motion is mainly dependent on the viscosity of the two fluids, temperature, and surface area of contact. The more the surface area, the faster the diffusion. To quantify the phenomena, the flux through the interface of the two liquids is proportional to the gradient of the concentrations of the liquids and is given by Fick's law as:

$$J = -D\frac{d\phi}{dx} \tag{1.1}$$

where J is the diffusion flux, D is the diffusion coefficient (or diffusivity), $d\phi$ is the concentration change and dx is the change in coordinate. Diffusivity represents the rate of movement of the mass due to thermal agitation of the molecules/atoms without bulk mass motion, which may be caused by the motion of one or more objects through various phases. The diffusivity depends on temperature, pressure, and surface morphology. Stirring, on the other hand, is the random addition of kinetic energy to the molecules of a fluid that leads to turbulence and variable velocities of particles at different space coordinates.

The diffusion equation can be derived from the Ficks's law as: Let time rate change of mass of 2 liquids be defined by change in flux at two positions as:

$$\frac{dM}{dt} = \mathrm{J(x_1,t)} \text{ - } \mathrm{J(x_2,t)}$$

$$\frac{dM}{dt} = \mathrm{D}(\frac{d\phi_2}{dx} \text{ - } \frac{d\phi_1}{dx})$$

But, we have M = Δx .ϕ(x,t), where ϕ is the concentration. Thus, we get:

$$\frac{d\phi}{dt} = \mathrm{D}(\frac{d\phi_2}{dx} \text{ - } \frac{d\phi_1}{dx})/\Delta x$$

Taking limit, $\Delta x \to 0$, we get the diffusion equation as:

$$\frac{d\phi}{dt} = D(\frac{d^2\phi}{dx^2}) \tag{1.2}$$

Eq(1.2) is for system in 1-D. For a system in 3-D, we have the equation given by:

$$\frac{\partial\phi(x_i,t)}{\partial t} = D\nabla^2\phi(x_i,t) \tag{1.3}$$

When there is a pressure gradient, it leads to flow in the system, leading to change in concentration in time with respect to concentration gradient. This phenomena is called convection. The phenomena equation is given by:

$$\frac{\partial \phi(x_i, t)}{\partial t} = -\beta \frac{\partial \phi}{\partial x_i} \tag{1.4}$$

Combining the diffusion and convections, we can get the equation of motion of fluids as:

$$\frac{\partial \phi(x_i, t)}{\partial t} = D\nabla^2 \phi(x_i, t) - \beta \frac{\partial \phi(x_i, t)}{\partial x_i} \tag{1.5}$$

For a steady state, we assume that the concentration doesn't change with time. Which means:

$$\frac{\partial \phi}{\partial t} = 0 = D\nabla^2 \phi(x_i, t) - \beta \frac{\partial \phi(x_i, t)}{\partial x_i}$$

Hence, for a steady state, we have:

$$\beta \frac{\partial \phi}{\partial x} = D \frac{\partial^2 \phi}{\partial y^2} \tag{1.6}$$

The solution of this equation is complex and is found to be extensively dependent on the diffusion coefficient. Suh et al. [5] reported a quantitative study on the time taken for mixing solutions with pure diffusion and convection. They reported that advection was an important process that made the mixing less dependent on diffusion coefficient and rather more on the geometry of the tube of mixing. Thus, advection helped in the rapid mixing of the solutions and lead to lower mixing times, compared to pure convection and diffusion.

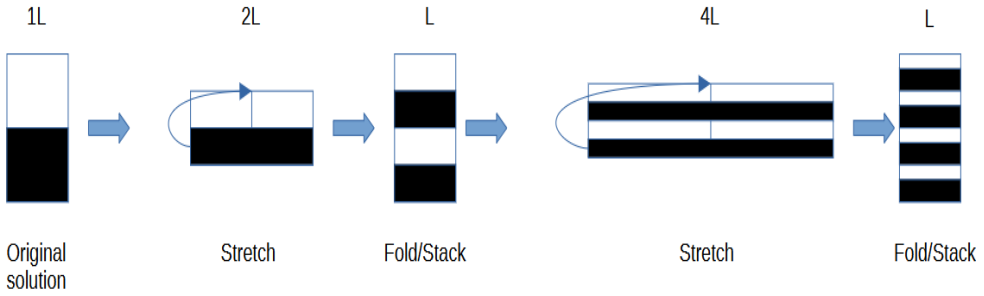

Figure 1.1: Baker transformation.

Advection is the movement of the particle dissolved or suspended in the fluid. For a system with advection in steady state, the equation of motion is given by:

$$\beta \frac{\partial \phi}{\partial x} + V \frac{\partial \phi}{\partial y} = D \frac{\partial^2 \phi}{\partial y^2} \tag{1.7}$$

where V is the squeezing velocity of striation. The effectiveness of mixing is measured through the average combined thickness of two layers or the separation of

two similar interfaces and is also a measure of the degree of segregation. This thickness, called striation thickness, is a distinctive quality of mixtures in laminar flow [6]. Thin striation thickness is a prerequisite for faster diffusion which can be achieved through chaotic advection, which is the stretching and folding of the fluid blobs resulting in exponential decrease in the striation thickness. The mechanism of thinning can be demonstrated through Baker's transformation as shown in figure 1.1.

WWith the decrease in the striation thickness, there is an increase in the length of the column of interest. Baker's transformation starts with stretching of the column of liquids while keeping the volume the same. Then there is intermixing by folding of the column in half. This continues until there is complete mixing of the two solutions. As evident, the area of contact is also an important parameter to achieve faster mixing. Thus, one can increase the efficiency of mixing through the use of multiple reservoirs/channels as inlets for mixing two liquids as it increases the surface area of contact and hence increases the diffusion. This decreases the time of mixing by order of (length)2 but, this can pose an issue if diffusion coefficient is very large and the number of channels for mixing can rise exponentially. Thus, advection-inducing channels are used extensively for mixing fluids.

1.1.1 Laminar flow

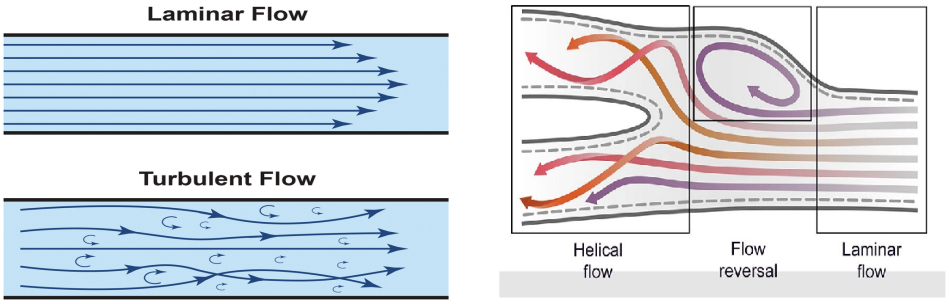

(a) Laminar Flow in a channel [7] (b) Types of flows in a channel[8].

Figure 1.2: Flows in a channel

Laminar flow can be described as the motion of a fluid where every particle in the fluid follows the same path as its previous particles, as shown in fig 1.2a. Since the microfluidics channels are very small, lamellar flows are observed. An important consequence of laminar flow is that two flows in contact mix through diffusion only. In the case of circular tubes, concentric fluid tubes with thin walls make up the laminar flow in the tube. The flow's velocity increases from zero at the tube wall to a maximum at the center line of the tube. There are no pressure gradients across the tube's diameter and the flow is directed along its axis. But, between each tube, there is a shear stress (τ) that grows by dτ for

each tube in the radial direction. This shear stress is balanced by there a pressure difference between the fluid tube's ends. The pressure gradient, $\Delta P/\Delta L$, along the axis is considered constant because if it were not constant, it will lead to a discontinuity in the pressure which would result in turbulence in the flow, leading to a non-laminar flow. There are various indications using which the properties of the fluid flows are characterized. These include: Reynold's number, Pecltet's number, Bijan number, Ericksen number etc. Most important of these are the Reynold's and Peclet numbers since they give an idea about the type of flow.

Reynold's number

Reynold's number is a measure of the ratio of inertial forces to viscous forces. It is an important parameter to determine whether a flow is turbulent or laminar. It is essential to find these parameters, especially in microfluidics, as fluids synthesized from low Reynold's number bearing flows (laminar flow) are reproduceable and have efficient mixing. Mathematically, the number is given by:

$$Re = \frac{LV_{avg}\rho}{\mu} \tag{1.8}$$

where L is most relevant length scale, V_{avg} is the average flow velocity, ρ is the density of fluid and μ is the viscosity. "Re" depends on three basic factors: material properties (density, viscosity), boundary conditions and critical velocities. A "Re" below 2300 is regarded as a laminar flow while an "Re" above 4000 is regarded as turbulent flow. Any intermediate numbers indicate a transient flow. In an microfluidics, the viscous forces dominate over the inertial forces, leading to lower Reynold's numbers. Thus, in microfluidics, we deal with highly laminar flows and hence, a higher reproducibility of results.

Peclet's Number

The peclet number is used in calculations of the convective heat transfers. It is the ratio of thermal energy which is convected to the fluid to the thermal energy which is conducted within the flow[9]. Mathematically, it can be expressed as:

$$Pe = \frac{heat_{convection}}{heat_{conduction}} \tag{1.9}$$

In terms of specific heats and densities:

$$Pe = R_e.P_r = \frac{\rho.C_P\Delta T/l}{k.\Delta T/l^2} \tag{1.10}$$

A large Peclet number indicates an advectively dominated distribution and a small number indicates a diffusive flow. The Peclet number measures the relative importance of advection versus diffusion.

1.2 Laws of heat and mass transfer

Fluid mechanics consists of three fundamental conversion concepts - mass, energy, and momentum - as well as the accompanying continuity equation, dynamic energy equation (Bernoulli's equation), and momentum equations. Their fundamental ideas are drawn from Laplace's law and Pascal's law [10]. The Pascal law states that: " Pressure or intensity of pressure at a point in a static fluid will be equal in all directions". The pressure that a static fluid exerts is known as static fluid pressure and results from the weight of the fluid, Hence, the pressure only depends on the fluid's depth (h), density (ρ), and gravitational acceleration (g). Mathematically, it is given by:

$$P_{static} = \rho g h \tag{1.11}$$

This equation is a special case of Navier's - Stokes equation where the viscosity and inertia terms are ignored [11]. The derivation of Navies stokes equation is tedious and not discussed in this report.

1.2.1 Mass Transfer (Continuity equation)

For cross-sectional area along a tube (A1 and A2) and having the same flow Q, it may be assumed that all of the fluid mass will steadily move through the tube. In other words, the mass of fluid traversing through each part of the pipe per unit time must be the same. Mathematically:

$$A_1 \rho_1 U_1 = A_2 \rho_2 U_2 \tag{1.12}$$

where $\rho_{1,2}$ are densities at different coordinates while $U_{1,2}$ are velocities of the fluid at the coordinates. This is very similar to the charge conservation equation and translates to the conservation of mass. Thus, in mass transfer, the mass is conserved.

1.2.2 Bernoulli's principle (Energy conservation)

Bernoulli's principle is a fundamental law in fluid mechanics. It is extensively studied and used in industries. Bernoulli's equation connects pressure, heights and speed of fluid to characterize the energy of the system. The Bernoulli's principle states that:" For viscous free fluid flow, an increase of the fluid velocity occurs simultaneously with a decrease in fluid pressure (ΔP) or a decrease in the fluid's potential energy". Mathematically, it is given as:

$$P + \rho g h + \frac{1}{2}\rho v^2 = const \tag{1.13}$$

where P is the static pressure, h the height, v the velocity, ρ the density of the fluid, and g the acceleration due to gravity at a given space coordinate. The Bernoulli's principle ignores the viscous forces which can result in deviations in actual experiments compared to theoretical calculations. Thus, a correction is generally included through Poiseulli's law.

1.2.3 Poiseulli's Law

The Poiseulli's law states that: "the velocity of a liquid flowing through a capillary is directly proportional to the pressure of the liquid and the fourth power of the radius of the capillary and is inversely proportional to the viscosity of the liquid and the length of the capillary". Mathematically, it is given as:

$$\Delta P = \frac{8Q\mu L}{\pi r^4} \tag{1.14}$$

where L is the length of the tube, Q is the volumetric flow rate, r is its radius, and μ is the dynamic viscosity of the fluid. Although this equation can be modified based on the geometry of the tube, it is a common phenomenon that change of pressure is directly proportional to the viscosity of the fluid. Also, if the walls are not smooth, a higher drop in pressure is observed than expected [12]. Analogous to resistance to electricity, a flow resistance can be defined as the ability of channels to resist the flow. The resistance for a circular channel is given by:

$$R = \frac{\Delta P}{Q} = \frac{8\mu L}{\pi r^4} \tag{1.15}$$

Thus, choosing the correct material for microchannels is essential to reduce resistance to the flows. The resistance is dependent of the surface wetting phenomena.

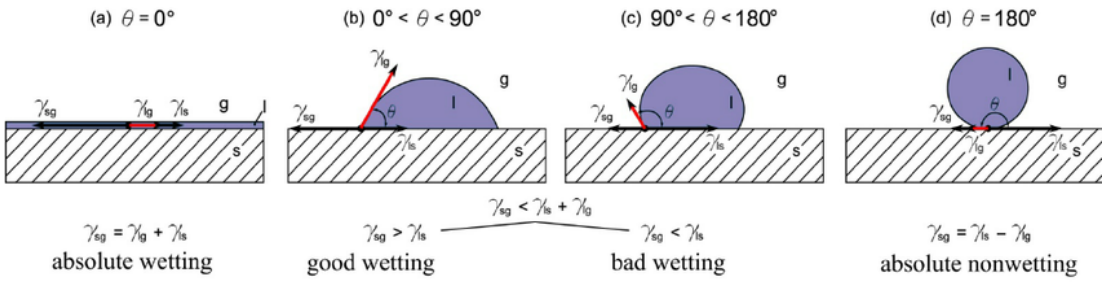

Figure 1.3: Wetting on surfaces [13].

Wetting is the ability of a material to maintain contact with liquid over a prolonged time due to molecular interactions between the two. The wetting capacity is generally characterized through surface contact angles. Contact angle is the angle between a tangent to the liquid surface and the solid surface at the point of contact. A surface with contact angle more than 90^o is defined as hydrophobic while a surface with the contact angle less than 90^o is termed as hydrophilic, as shown in fig:1.3. This occurs due to the difference of surface tension of the liquid - gas - solid interface. A hydrophilic surface leads to resistance in flow since there is interaction between the surface and the liquid. Thus, a hydrophobic material is used for crafting microfluidics channels.

1.2.4 Surfactant in microfluidics

The surface tension is a measure of the energy stored in the interface. This arises due to cohesion between liquid molecules at the interface. Molecules with high surface tensions tend to close in and come in contact with other neighboring molecules to reduce the surface energy and stabilize. A surfactant is a chemical that reduces the surface tension of a liquid. Some common examples include soaps, detergents etc. These reduce the surface tension at the oil - water interface, thus stabilizing the mixture. Through surfactants, non - wetting materials can be made partially or completely wetting due to reduction in the surface tension. Surfactants affect the wetting behavior of hydrophobic materials to lower the interface free energy by adhering to the liquid-vapor, solid-liquid, and solid-vapor interfaces. The polar head groups of surfactants,that are absorbed onto hydrophobic surfaces, face into the solution with the tail pointing outside and make it hydrophilic. Surfactants such as Polyvinyl alcohol (PVA), Sodium stearate, etc are often used to stabilize nanoparticles when they're in unstable in a medium. These surfactants reduce the surface tension of nanoparticles, thus their energies are reduced, leading to dispersed particles and hence reducing the size.

1.3 Effect of geometry in microfluidics

Microfluidic mixing can be divided into two categories: active mixing and passive mixing [14], as shown in fig 1.4. Passive mixing is use of different techniques,such as changing the design or arrangement of fluid channels, to achieve efficient mixing of fluids. This kind of mixing is built into the system during fabrication and is not managed by users outside the system. The main advantage of passive mixing is that there are no moving elements in the mixer, making it simpler to construct and use. As discussed before, the geometry of the fluidics channels induce advection which is essential for faster and efficient mixing. Thus, choosing a geometry of channel is an important prerequisite for mixing fluids through microfluidics.

Active mixing consists of using mechanical methods to induce mixing. One can activate an active mixer when needed, and controllable mixing can be done with the help of pressure gradients, electrical voltages applied across the fluid, or built-in mixing components like stirring bars. They typically improve mixing by mechanically, magnetically, electrically, or acoustically stirring the fluid. Although active mixers can improve mixing, especially for chamber mixing, they are more difficult to make than passive mixers because they have moving parts and frequently need an external power source. methods to improve mixing efficiency through passive efficiency is discussed.

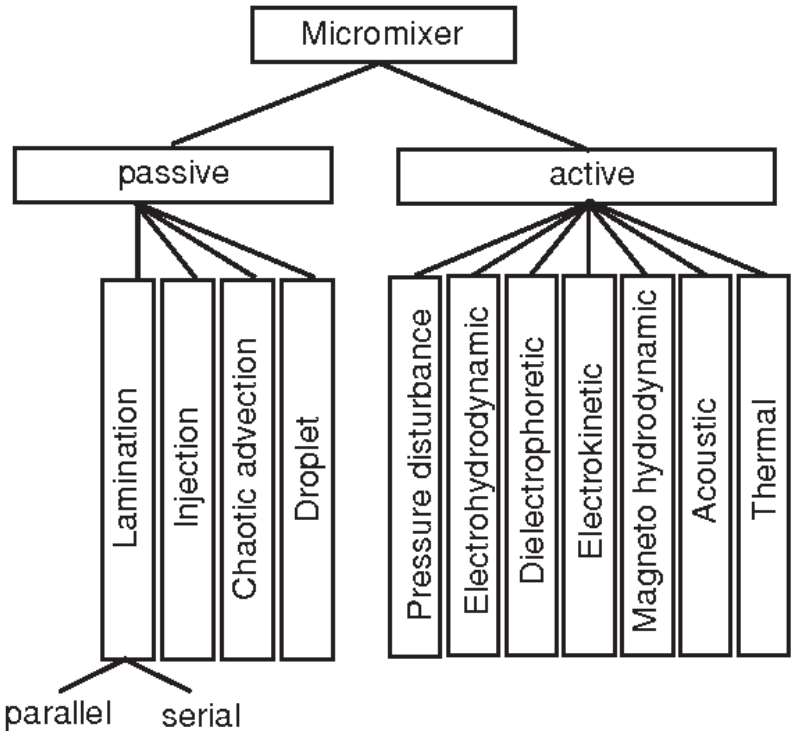

Figure 1.4: Types of micromixers [15].

1.3.1 Splitting the channels

When mixing occurs, the two streams are combined into one channel during the first step. The two fluids then diffuse across the interface, resulting in a molecular mixture that is uniform. Due to Brownian and random motion along the concentration gradient between the two fluids, mass and heat are transported in this situation. The diffusion occurs more quickly across the long interface between the two fluids when the number of interfaces increase, increasing the area of contacct. Due to a high Peclet number, this process is generally very slow in microfluidic devices. Figure 1.5 depicts the mixing procedure in a microfluidic device by joining two channels into a single channel. For full mixing to occur in such a device, a long channel is necessary.

By reducing the mixing path by twisting the inlet streams or using complex geometries, a conventional T- or Y-shaped mixer can be improved. To improve mixing even more, streams that have already been combined can be split and then recombined in series. To mix multiple parallel streams, they can be combined in a T-shape, and with the right design, 3D flows can even be created inside of microfluidic devices. However, these variations necessitate a more challenging channel fabrication process, which raises the price of the device.

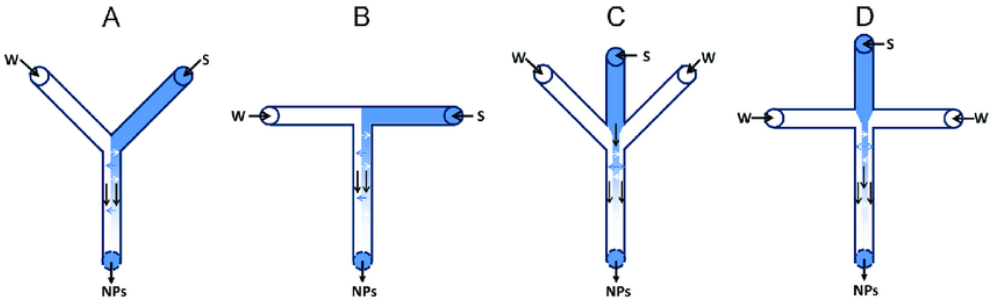

Figure 1.5: Mixing of two fluids in different mixers, (A), T-shape microfluidic mixer (B), planar flow focusing mixer (C) and cross-shaped planar flow focusing mixer (D) [16].

1.3.2 Microchannel modifications

Slanted wells are a type of passive mixer that can provide additional mixing within the system without lengthening the overall channel length. They are a relatively simple passive mixer to fabricate within a microfluidic device. These mixers are modern enhancements to the conventional stream splitting technique for improving mixing in microfluidics. By increasing the amount of lateral transport within the channel, researchers have attempted to increase the mixing rate beyond what would be attained by diffusion alone, theoretically reducing the mixing distance. Stroock et al. [18] used oblique ridges to create a passive mixer for microfluidic devices. They proposed the theory that "stirring flows," or flows with transverse components that fold fluid components over the cross-section of a channel, result in chaotic advection within the flow, which in turn improves mixing. In essence, the fluid streams stir into one another as a result of the traverse flows that are created. This chaotic flow was produced by Stroock et al. by repeatedly combining rotational and extensional flows. Patterned grooves are incorporated into this passive mixer on the channel floor. The staggered herringbone structure, as shown in fig 1.6, of these patterned grooves allows for even better mixing enhancement than the slanted wells.

Due to the lack of moving parts, passive mixers with patterned grooves enable improved mixing within a microfluidic channel without the need for an external power source or complicated microfabrication techniques. When using patterned grooves, the channel length necessary for complete mixing can be drastically reduced if the grooves are deep enough. These grooves do have a disadvantage, though, in that they cause dead volume in the channel. Dead volume is the volume of the of the fluids that is out of the flow path. In other words, it is not recovered after microfluidics. To further the advancements in mixing enhancement achieved by using this type of groove, more research on reducing or eliminating this dead volume should be conducted.

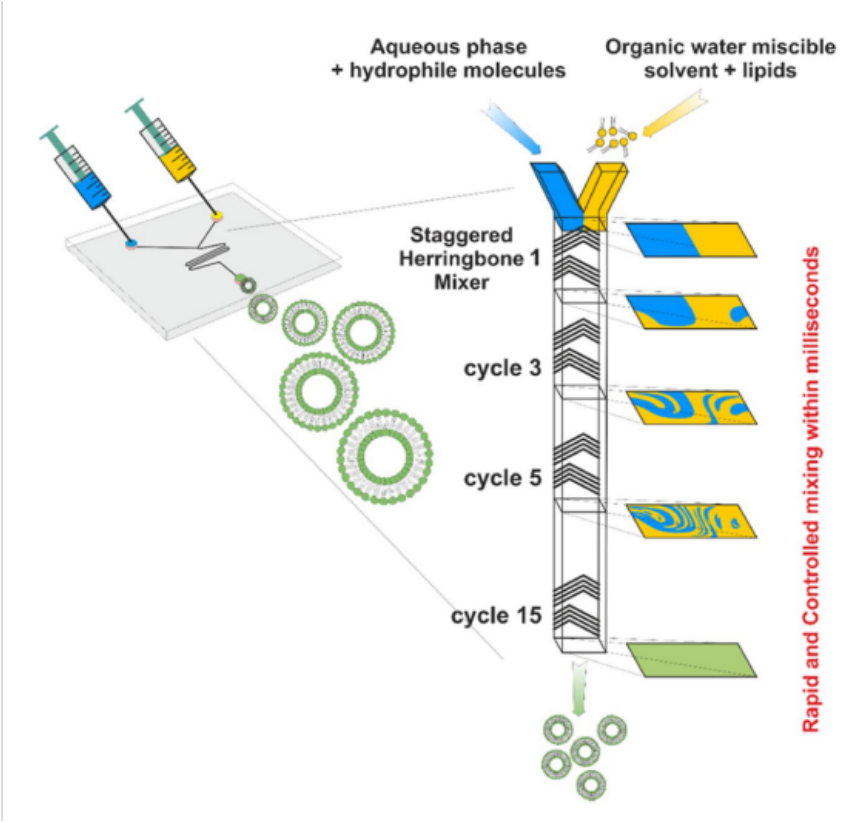

Figure 1.6: Mixing of two fluids in staggered herringbone channel [17].

1.4 Microfluidic parameters

The Total flow rate (TFR) is defined as the summation of flow rates of the fluids through the aqueous and the organic phases. A higher flow rates means, the fluids move faster through a channel. The Flow rate ratio (FRR) is defined as the ratio of flow rates through the aqueous and the organic phases. A higher FRR suggests that the difference between speeds of the two phases is high. A FRR of 1 means that the aqueous and the organic phases move at same speeds. With an increase in the FRR, the polarity of the solution increases, leading to faster nanoparticle sheets formation and hence faster folding. Since the polymers are folded faster, a large growth of the particles is not observed leading to smaller particles. Since all the polymers face the repulsion of aqueous phase, most of the polymers are folded at initial stages of mixing leading to uniform size and lower PDI values. Since folding is a kinetic process, the drug encapsulated inside the nanoparticles does not leak out easily due to strong intermolecular forces between the polymer molecules and non-rearrangement of the nanoparticles.

The encapsulation is quantified through encapsulation efficiency (EE). It is the percentage of the drug that is entrapped inside the nanoparticle. Mathematically,

it is given by:

$$EE(\%) = \frac{M_{total} - M_{sup}}{M_{total}}.100 \tag{1.16}$$

where M_{total} is the net drug added in the synthesis and M_{sup} is the drug in the supernatant after centrifuge. Another parameter, loading capacity (LC) is used to characterize the encapsulation. It is defined as the percentage of the loaded drug per unit mass of the nanoparticle. Mathematically, it is given by:

$$LC(\%) = \frac{M_{total} - M_{sup}}{M_{np}}.100 \tag{1.17}$$

where M_{np} is the mass of the nanoparticles.

Size in nanoparticles is important parameter since, a larger nanoparticle entraps more drugs. Also, the cell uptake of nanoparticles is size dependent. The smaller the nanoparticle, the better it is uptaken by the cells [19] . Size of nanoparticles can be used to target specific sites for treatment. Also, in order to reach cellular level uptakes, the sizes are required to be in range of 20-200 nm. Along with this, the uniformness of the nanoparticle sizes is essential for uptake efficiency. A non uniform solution of nanoparticles cannot be target specific. The size uniformness is measured through a dimensionless number called polydisperity index (PDI). PDI is a number ranging from 0 - 1, where 0 depicts a highly monodispersed nanoparticles, while a higher number indicates non-uniform distribution of sizes of particles.A highly monodispersed sample is a stable emulsion as the particles have enough intermolecular forces to repel each other and increase the intermolecular spaces, thus resisting agglomeration and decrease the overall size.

Nanoparticle synthesis is a tedious and long process. These can be prepared though various techniques such as sputtering, co-emulsification, laser ablation etc. But these techniques often lead to inconsistencies in the synthesis. Often, the industries struggle with synthesis due to these inconsistencies. Microfluidics is a novel approach to synthesize nanoparticles due to its reporoducibility and robustness. It also requires minimal interference from human, thus reducing the human errors too. Microfluidics are performed at small scales and also reduce the wastage of resources. Hence, in this report, synthesis of nanoparticles through microfluidics was studied.

1.5 PLGA Nanoparticles

PLGA is a biodegradable polymer that is extensively used in drug delivery. It is a copolymer of poly lactic acid (PLA) and ply glycolic acid (PGA) in different ratios. PLGA is found in various forms, PLGA 50:50, PLGA 85:15, PLGA 75:25, based on the ratio between the PLA and PGA polymers [20]. The PGA is more hydrophilic in nature compared to PLA. Thus, PLGA with higher PGA concentration is hybdrophilic. PLGA is efficiently taken up by the cells and utilized

over a long time due to its stability. The PLGA polymer degrades through hydrolysis within the body, thus a drug encapsulated inside such polymer allows for sustained drug release [21][22]. Further, PLGA does not affect the working of the dendritic cells (DC) in their cytokinin functioning or migration and maturation of DC, making it an apt candidate for drug delivery.

PLGA is generally dissolved in organic solvents such as acetonitrile (ACN), dimethylsulfoxide(DMSO), dimethylformamide (DMF), chloroform etc. The hydrophobicity of PLGA is an important property for synthesis of nanoparticles. When the organic phase comes in contact with an aqueous phase, it tries to minimize the area of contact to hydrophobic groups. Thus, the PLGA particles make long sheets with hydrophobic ends together and hydrophilic ends protruding in the aqueous phase, making PLGA somewhat stable. This again undergoes rapid changes in order to minimize the surface energies, thus the chain starts to curve and make closed loops. Closed loops have lower surface energies and increase the stability of the nanoparticles. When there is a drug in the mixture, the drug is encapsulated while the formation of the closed loops. A good example of such nanoparticles is liposomes. They are lipoprotein bilayered vesicles that can entrap various drugs for drug transport [23].

1.5.1 Microfluidics in PLGA nanoparticle synthesis

PLGA nanoparticles are encapsulated with desired drug for the drug delivery. The encapsulation amount is an important parameter in drug delivery. It is entirely dependent on the fabrication process and can be changed by varying parameters of synthesis. These parameters include TFR, FRR, end and start volumes, concentration of polymer, concentration of proteins, etc. This study was an attempt to standardize the process if nanoparticles synthesis for producing nanoparticles.

Chapter 2

Work Done

2.1 Experimental setup

2.1.1 Microfluidics

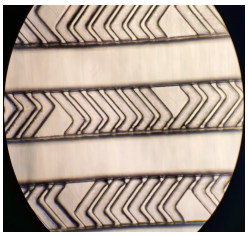

(a) Stagerred herringbone structure inside cartridge.

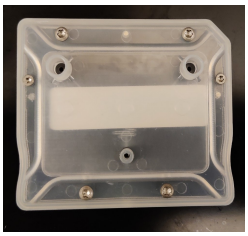

(b) Stagerred herringbone cartridge.

(c) Benchtop Nano Assemblr

Figure 2.1: Parts of a microfluidics

A Benchtop NanoAssemblr microfluidics system was used for preparation of nanoparticles. It uses a stagerred herringbone cartridge, using which aqueous and organic phase liquids are injected. The cartridge has two inlets, where syringe containing aqueous and organic phases are inserted. As the machine is run with defined parameters, viz, TFR, FRR, end and start volume, the pistons push the syringe plunger with constant speed that gives rise to flow in the cartridges. Inside the cartridge, mixing of organic and aqueous phase occurs within herringbone channels, thus formulation nanoparticles. These nanoparticles are then collected in a collection tube. The start and end volume are waste volumes that are collected in tube.

2.1.2 Zeta Sizer

A Malvern Nano-ZS was used for measurement of sizes as previously described by Joshi et al [25]. It uses dynamic light scattering in Brownian motion to get the sizes of the particles. It can also be used to measure the zeta potential. By

Figure 2.2: Malvern Zetasizer [24]

measuring the speed at which particles and molecules are moving as a result of electrophoresis, the charge or zeta potential of these entities is determined. If a field is provided, zeta potential particles and molecules will move in the direction of the electrode. The zeta potential and field strength both affect how quickly they move. If the field strength is known, the speed of movement is measured using laser Doppler electrophoresis, and then proven zeta potential theories are applied.

2.1.3 MicroBCA protein Assay

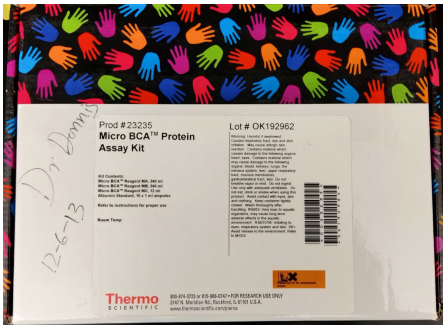

Figure 2.3: MicroBCA assay kit

A Thermo scientific microBCA assay kit containing reagents and Bovine serum albumin (BSA) protein (2mg/mL) as standard was used for testing the concentration of protein in the nanoparticles [26]. It uses a calibration table between optical density and known concentration of the BSA protein (0.5 to 200 μg/mL). The absorbance is calculated using the Beer Lambert's law, which states that "the absorbance of a solution is directly proportional to the concentration of the absorbing material present in the solution and path length". Thus, using the absorbance the concentration of the samples are calculated, which are used to find the net protein content in the samples.

2.1.4 Methodology

Nanoparticle synthesis

- PLGA organic phase was made with Acetonitrile (ACN) with concentration 10 g/L.
- Tris buffer solution was made with concentration of 10mM and pH 7.4. Polyvinyl alcohol (PVA) solution (1% w/v) was with de-ionized water.
- PVA + Tris solution with 3:2 (PVA : Tris) was made using existing solutions and is used as aqueous phase.
- BSA protein were added with different concentration in the aqueous phase.
- Microfluidics (Benchtop Nano Assemblr) was used to make nanoparticles, with FRR (Aq:Org) - 1:1 and TFR - 10 mL/min.
- Size and PDI were determined using DLS based zetasizer (Malvern Nano - ZS).

Nanoparticle synthesis calibration

- Start and end volumes were calibrated through hit and trials.
- The nanoparticles were synthesized in Tris buffer, but showed agglomeration after synthesis. Thus, PVA was added to stabilize the solution.
- Samples made with 10mL syringes were not apt for microfluidics due to backflow of solvents into the syringes.

MicroBCA

- Samples were weighed $\sim$ 10mg and 500 μL of 0.1N NaOH + 2% SDS solution was added and kept overnight at room temperature to dissolve the nanoparticles.
- The samples were centrifuged @ 13000 xg and then the supernatant was used for quatification of protein using microBCA kit.
- The BSA was diluted with PBS to different concentrations in order to get a calibration curve for absorbance vs concentration.
- Samples along with the diluted BSA were added into a 96 well plate. The plate was covered with a microplate adhesive tape and kept at 37^{o}C for 2 hours in a humidified chamber. Absorbance was measured at 562 nm.
- The samples were run in a microplate spectrophotometer (Epoch, BioTek , USA) to obtain absorbance for the samples.The calibration curve was plotted and the amount of protein in each sample was calculated. Using this, the encapsulation efficiency and loading capacity were calculated.

2.2 Results and discussion

Two polmers, viz PLGA 50:50 and PLGA 85:15 were used for the study. These polymers are relatively hydrophobic and have long shelf lives. The particles were produced according to the following table 2.1:

PLGA + ACN					
Serial No	Total Flow Rate (mL/min)	Flow Rate Ratio (FRR)	Total Volume (mL)	Left Syringe (Aqueous)	Right Syringe (Organic)
1	5	1	1	1	1
2		3	1	1	1
3		5	1	1	1
4	10	1	1	1	1
5		3	1	1	1
6		5	1	1	1
7	15	1	1	1	1
8		3	1	1	1
9		5	1	1	1

Table 2.1: Table for preparation of PLGA

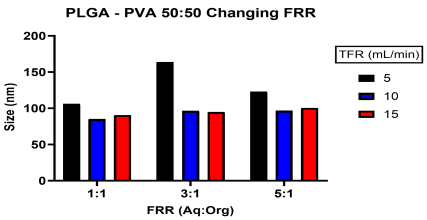

(a) Size of PLGA 50:50

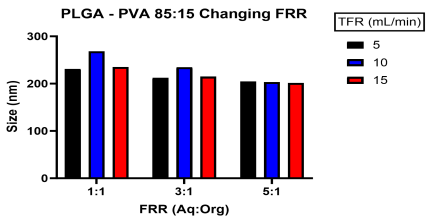

(b) Size of PLGA 85:15

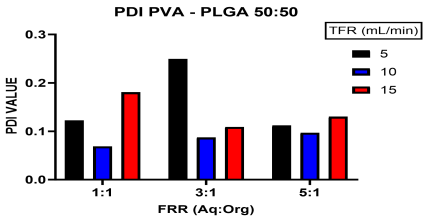

(c) Size of PLGA 85:15

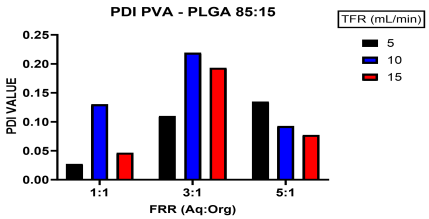

(d) PDI of PLGA 85:15

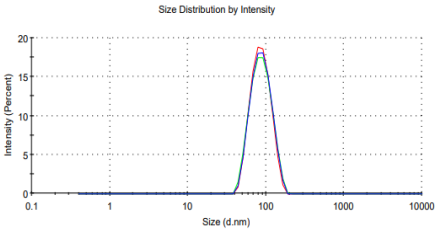

(e) Size distribution of PLGA 85:15

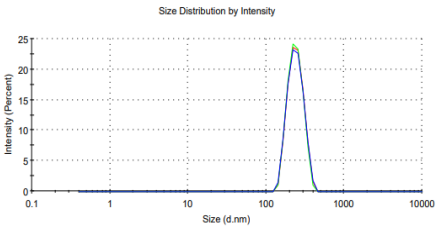

(f) Size distribution of PLGA 85:15

Figure 2.4: Size and PDI of Nanoparticles

The start waste volume was set at 0.35 mL and the end volume was set at 0.05 mL. After running the experiment, a general high PDI (¿0.35) was observed (results not reported here). Through prior experience, it was understood that the starting and ending volumes affect the overall PDI. The fluids at start tends to

flow through a channel which doesn't contain fluid. Thus, while flowing it also wets the surfaces and the surface forces interact with the starting columns of the fluids. This can result in turbulence and lead to a general higher PDI. Thus, the start and end volume were changed to 0.4 mL and 0.1 mL respectively. Nanoparticles were re-synthesized according to 2.1. Particle sizes were measured at room temperature and the results are reported in fig 2.4a and 2.4b. The PDI was also measured and reported in fig 2.4c and 2.4d. The PDI was below 0.1, showing highly mono dispersed samples. The size distribution graph, figure 2.4e and 2.4f, also shows that the particles have single peaks, showing lower PDI and an uniform distribution. Thus, the samples were stable with the desired size.

PLGA 50:50, with TFR - 10mL/min and FRR - 1:1 showed comparatively better results than the PLGA 85:15 samples, thus, PLGA 50:50 with the given TFR and FRR was used for rest of the standardization experiment. It was found that while preparing the nanoparticles, the solution was transparent but after freezing overnight a slight turbidity was observed. Thus, it was predicted that nanoparticles agglomerated after freezing. When the temperature is lowered, the random motion of particles reduces due to reduction in thermal agitations. Thus, the particles settle down and come close to each other. In doing so, they come in contact and agglomerate to reduce the overall surface energies, which was earlier compensated by thermal agitation. In order to prevent agglomeration, PVA was used in the initial stages of the experiment. The addition of PVA is discussed in the methodology of nanoparticle synthesis. Nanoparticles were prepared with the use of PVA, following the table 2.2, along with a test to see the effect of two different methods of addition of PVA along with the effect of freezing.

PLGA (50:50) + ACN										
Serial No	Total Flow Rate (mL/min)	Flow Rate Ratio (FRR)	Total Volume (mL)	Left Syringe (Aqueous)	Right Syringe (Organic)	PVA (Aqueous phase)	PVA_tube	Aq Value	Org Vol	PVA_percentage
501	5	1	2	1	1	0	0.75	1	1	0.25
502	10	1	2	1	1	0	0.75	1	1	0.25
503	15	1	2	1	1	0	0.75	1	1	0.25
504	5	1	2	1	1	0.5	0	1	1	0.25
505	10	1	2	1	1	0.5	0	1	1	0.25
506	15	1	2	1	1	0.5	0	1	1	0.25

Table 2.2: PLGA with PVA

The PVA was added through two methods given as:

- Addition of PVA (1%) to aqueous phase with a net 0.33% w/v final solution.
- Addition of PVA (1%) by direct addition in the collection tube, making a final 0.33% w/v solution

It was observed that there was an increase in the size of nanoparticles when the PVA was added into the collection tube after microfluidics as shown in figure 2.5a. Also, a higher PDI was (not reported) observed when PVA was added in the samples after microfluidics. Thus, in further preparation, PVA was used in the aqueous phase for the synthesis of nanoparticles. Further, the effect of

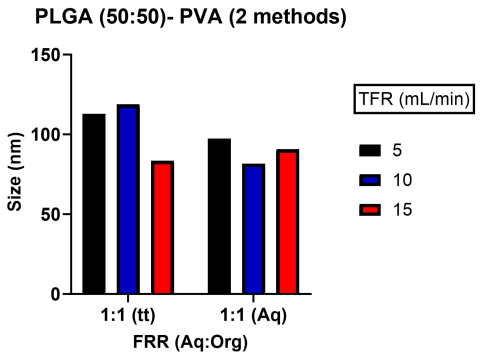

(a) Size of PLGA 50:50 via addition of PVA through the two methods

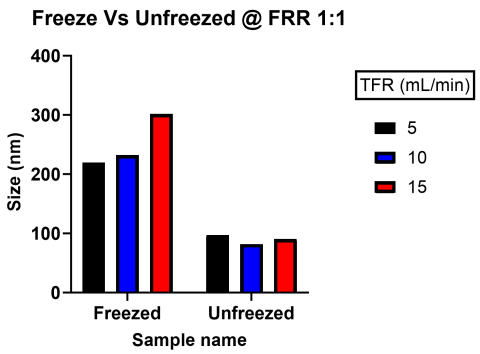

(b) Size of PLGA 50:50 before and after freezing

Figure 2.5: Addition of PVA

freezing was studied. It was observed that after freezing, the sizes of the nano particles increased by upto 3 times, as shown in figure 2.5b, showing coagulation of particles after freeze and thaw. In order to solve this issue, a cryoprotectant must be used to stabilize the sizes. Trehalose 5% solution was used as a measure to retain the sizes of the nanoparticles after freezing. For studying the nature of PLGA 85:15, the same experiment was done with the addition of PVA followed by by size and PDI analysis. Interestingly, the results obtained were opposite to what obtained with PLGA 50:50, as shown in figure 2.6. This could be due to higher hydrophobic nature of PLGA 85:15.

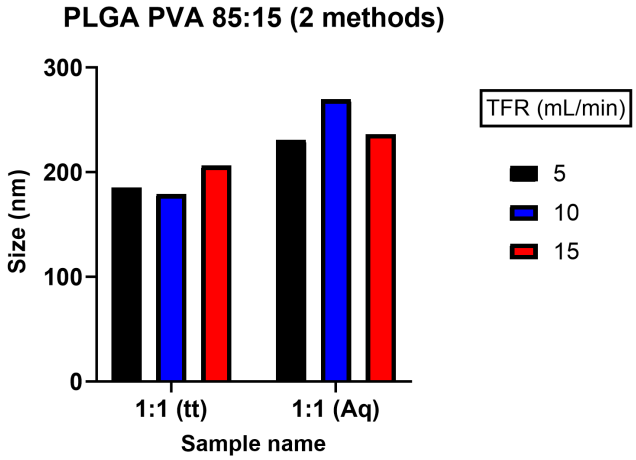

Figure 2.6: Two methods of addition of PVA

After obtaining the nanoparticle characteristic table without proteins, Albumin (BSA) protein was added to the aqueous phase for encapsulation in the nanoparticles. BSA is a hydrophilic protein which dissolves easily in water. Through the characteristic table formulation, TFR - 10mL/min and FRR - 1:1 was chosen to synthesize the nanoparticles. BSA was added to aqueous phase with different

concentrations of 0.1mg/mL 0.2 mg/mL, 0.5 mg/mL and 1mg/mL. Samples were made using the methodology mentioned in Nanoparticle synthesis. The size of nanoparticles was measured after their preparation and the results are reported in figure 2.7.

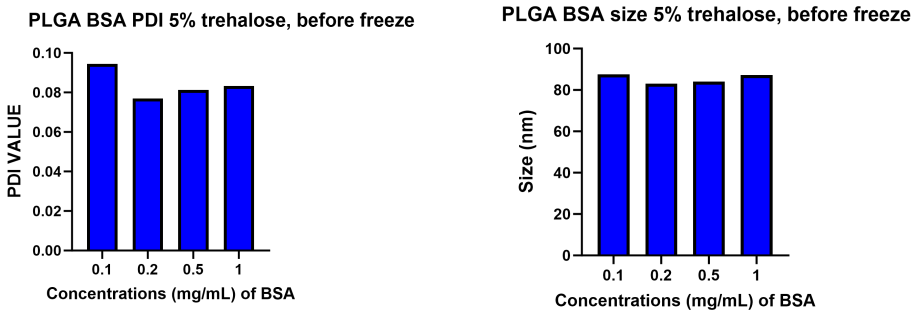

(a) PDI of PLGA BSA before freezing

(b) Size of PLGA BSA before freezing

Figure 2.7: Size and PDI of nanoparticles.

It was observed that addition of proteins did not change the size of the nanoparticles, as shown in figure 2.7b. This shows that proteins do not affect the size of particles drastically. The PDI values were also found to be less than 0.1 and in range of empty nanoparticles, showing that the nanoparticles are uninfluenced by the encapsulation of a protein, as shown in fig 2.7a.

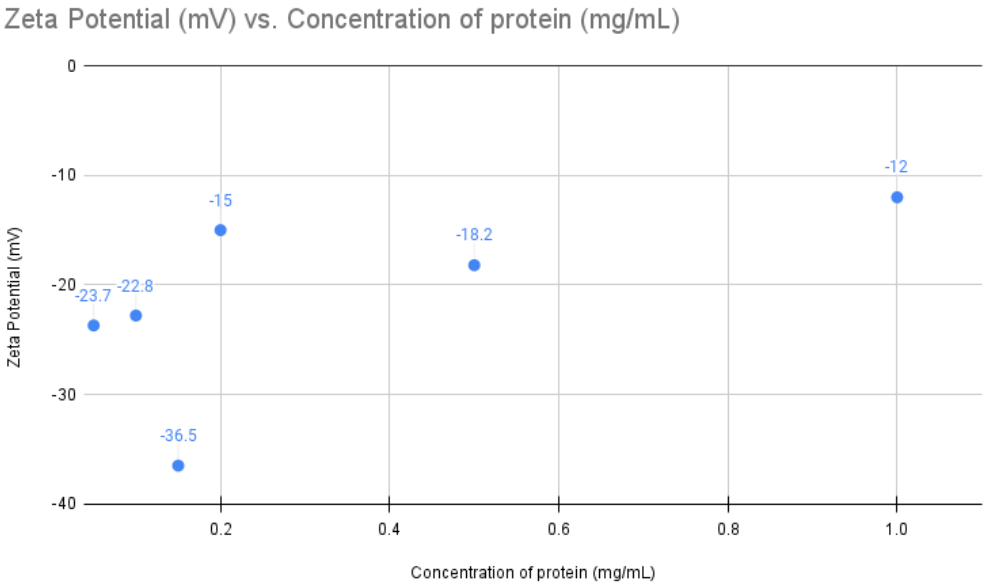

Figure 2.8: Zeta potential vs concentration of BSA protein

Next, the zeta potential was measured to determine the stability of the nanoparticles. A solution with absolute zeta potential more than 30 mV is termed as stable and does not coagulate over time. The zeta potential, as shown in figure 2.8, depicts that the samples had similar zeta potentials. The zeta potential of the samples was in range of -12 mv to -35 mV. A change of 20 mV is not regarded as huge. This showed that changes in amount of protein brought minor changes to the zeta potential, thus the properties of the nanoparticles were not drastically changed with addition of a protein.

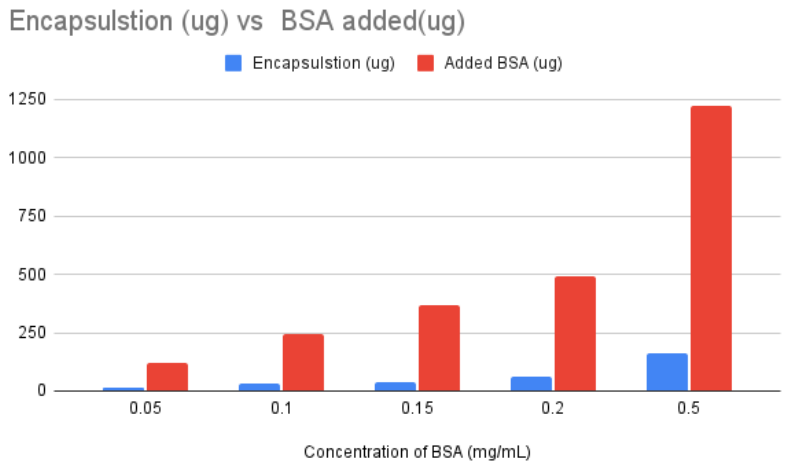

Figure 2.9: Encapsulation through varying BSA concentrations.

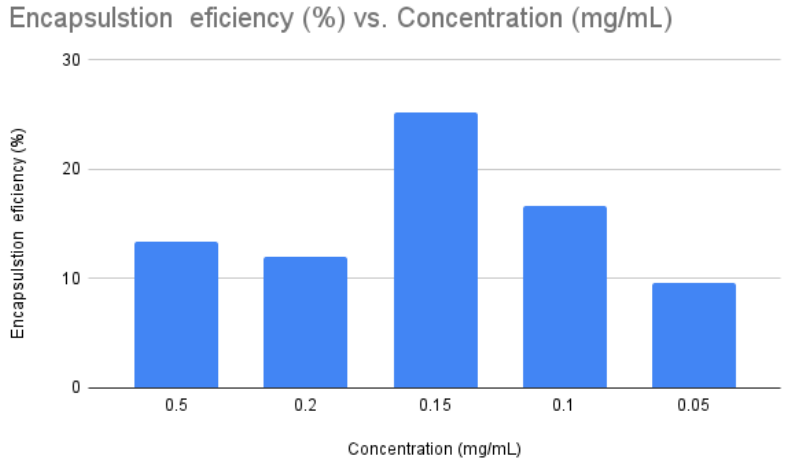

Figure 2.10: Encapsulation efficiency

MicroBCA was finally done to assess the EE% and LC%. The encapsulation was found to be in range of, as shown in fig 2.9. It shows that as the amount of proteins increased, the encapsulation increased. However, the best EE was obtained for 0.15 was a good (or bad) encapsulation in the nanoparticles. It shows that the

encapsulation increased with the increase in the total protein contents. But, the ratio of encapsulated protein and total protein follows a delta function. It tapers down the edges while it reached maxima in the center, as shown in figure 2.10. This shows that 0.15 mg/mL protein is the apt concentration for BSA loaded nanoparticle synthesis.

Hydrophilic drugs are less susceptible to encapsulation compared to hydrophobic drugs [25]. Hydrophobic are repelled by water, thus they are pushed into between the nanoparticles as much as possible to reduce contact with aqueous media. This is not true for hydrophilic drugs. Thus, encapsulation of drugs can be enhanced by attaching hydrophobic groups to the drugs. In the experiment, BSA encapsulated nanoparticles were formed using microfluidics with size less than 100 nms. The nanoparticles showed uniform distribution along with a stable suspension and can be used for further studies.

Chapter 3

Future Work

Using BSA protein as a model system, the current study has provided valuable insights into microfluidics-enabled nanoparticle synthesis and encapsulation. Future research endeavors can expand and delve deeper into several promising directions by building on this foundation.

Protein Variation and Encapsulation Properties: Exploring the encapsulation potential of different proteins, such as rMOMP, has enormous potential for broadening the applicability of microfluidic-synthesized nanoparticles. Investigating their interactions with the polymer matrix and determining how differences in protein properties affect encapsulation efficiency may lead to the development of tailored nanoparticle systems for specific therapeutic or diagnostic applications.

Hydrophobic Protein Encapsulation: The possibility of increased encapsulation efficiency with more hydrophobic proteins opens up a fascinating line of inquiry. Systematic studies with a variety of hydrophobic proteins can validate and quantify this trend, providing opportunities for microfluidic parameter optimization and fine-tuning to achieve even higher encapsulation yields.

Surface Characterization Techniques: Using advanced surface characterization techniques such as electron microscopy, FTIR, and AFM, you can gain a thorough understanding of the nanoparticle morphology, structure, and surface chemistry. These findings can be used to guide the development of nanoparticles with desired properties and functions.

Drug Release Kinetics: Examining the release profile of encapsulated compounds under different conditions, such as pH or temperature, can provide critical information about the nanoparticles' controlled release behavior. This understanding is critical for designing drug delivery systems with precise release kinetics.

Multifunctional Nanoparticles: Future research could look into incorporating additional functionalities, such as targeting ligands or imaging agents, into

the synthesized nanoparticles. This could pave the way for new theranostic applications in which diagnosis and therapy are combined in a single nanoparticle-based system. Transitioning from in vitro to in vivo models is a critical step in translating microfluidic-synthesized nanoparticles into practical applications. Biocompatibility, biodistribution, and therapeutic efficacy will be assessed in relevant animal models, providing valuable data for clinical translation.

In the end, one can unlock the full potential of microfluidics in nanoparticle synthesis and advance the field's contributions to biomedicine, materials science, and beyond by addressing these future research avenues.

Chapter 4

Conclusion

This comprehensive report has illuminated the usefulness of microfluidics as a pioneering science and technology, demonstrating its potential in microfluidics fluid manipulation. This study has highlighted the importance of standardized factors such as flow rate ratio, total flow rate, and polymer concentration in achieving precise encapsulation of BSA through a meticulous exploration of the synthesis of sub-100nm nanoparticles using the PLGA polymer.

The nanoparticles were stable and formed highly dispersed suspension. The average sizes of the nanoparticles ranged from 82- 87 nm. The PDI was also low ~ 0.1 showing that nanoparticles had uniform sizes. Further, zeta potential investigations show that the samples had zeta potential in 24 - 35 mV range, which is apt for a stable suspension without much deviations in the zeta potential, showing similar properties of the particles. The graphical representation highlighted key relationships, which improved comprehension. The implications are far-reaching, with promising advances in drug delivery, diagnostics, and materials science. This study, as a beacon for future research, highlights microfluidics' transformative impact, fueling innovation across multidisciplinary landscapes. The journey continues, with this report marking an important step forward in the ongoing investigation of microfluidic capabilities.

References

[1] Gregory A. Cooksey, John T. Elliott, and Anne L. Plant. "Reproducibility and Robustness of a Real-Time Microfluidic Cell Toxicity Assay". In: *Analytical Chemistry* 83.10 (Apr. 2011), pp. 3890–3896. DOI: 10.1021/ac200273f. URL: https://doi.org/10.1021/ac200273f.

[2] David Wibowo, Chun-Xia Zhao, and Yinghe He. "Fluid properties and hydrodynamics of microfluidic systems". In: *Microfluidics for Pharmaceutical Applications*. Elsevier, 2019, pp. 37–77. DOI: 10.1016/b978-0-12-812659-2.00002-8. URL: https://doi.org/10.1016/b978-0-12-812659-2.00002-8.

[3] Alexander Lobasov and Andrey Minakov. "Density effect on the mixing efficiency and flow modes in T-shaped micromixers". In: *MATEC Web of Conferences* 115 (2017). Ed. by S.V. Alekseenko, p. 07002. DOI: 10.1051/matecconf/201711507002. URL: https://doi.org/10.1051/matecconf/201711507002.

[4] Hassan Aref. "Stirring by chaotic advection". In: *Journal of Fluid Mechanics* 143 (June 1984), pp. 1–21. DOI: 10.1017/s0022112084001233. URL: https://doi.org/10.1017/s0022112084001233.

[5] Yong Kweon Suh and Sangmo Kang. "A Review on Mixing in Microfluidics". In: *Micromachines* 1 (3 Sept. 2010), pp. 82–111. ISSN: 2072-666X. DOI: 10.3390/mi1030082. URL: http://www.mdpi.com/2072-666X/1/3/82.

[6] W. D. Mohr, R. L. Saxton, and C. H. Jepson. "Mixing in Laminar-Flow Systems". In: *Industrial and Engineering Chemistry* 49 (11 Nov. 1957), pp. 1855–1856. ISSN: 0019-7866. DOI: 10.1021/ie50575a030.

[7] Abtin Ameri. "Improving the Numerical Stability of Higher Order Methods with Applications to Fluid Dynamics". PhD thesis. Dec. 2019. DOI: 10.13140/RG.2.2.25335.78247.

[8] Jim Baun. "Emerging Technology: Ultrasound Vector Flow Imaging - A Novel Approach to Arterial Hemodynamic Quantification". In: *Journal of Diagnostic Medical Sonography* 37.6 (July 2021), pp. 599–606. DOI: 10.1177/87564793211036013. URL: https://doi.org/10.1177/87564793211036013.

[9] Sandeep Arya et al. "Microfluidic Mechanics and Applications: a Review". In: 2013.

[10] Yujun Song et al. “Fundamental Concepts and Physics in Microfluidics”. In: *Microfluidics: Fundamental, Devices and Applications*. Wiley-VCH Verlag GmbH and Co. KGaA, Jan. 2018, pp. 19–111. DOI: 10.1002/9783527800643.ch2. URL: https://doi.org/10.1002/9783527800643.ch2.

[11] Cambridge Philosophical Society. *Transactions of the Cambridge Philosophical Society*. Vol. Vol. 8. https://www.biodiversitylibrary.org/bibliography/2348. 1849, p. 772. URL: https://www.biodiversitylibrary.org/item/49441.

[12] “Physics and Applications of Microfluidics in Biology”. In: *Annual Review of Biomedical Engineering* 4 (1 Aug. 2002), pp. 261–286. ISSN: 1523-9829. DOI: 10.1146/annurev.bioeng.4.112601.125916.

[13] Frantisek Pochly et al. “Study of the Adhesive Coefficient Effect on the Hydraulic Losses and Cavitation”. In: *International Journal of Fluid Machinery and Systems* 3 (4 Dec. 2010), pp. 386–395. ISSN: 1882-9554. DOI: 10.5293/IJFMS.2010.3.4.386.

[14] Hengzi Wang et al. “Numerical investigation of mixing in microchannels with patterned grooves”. In: *Journal of Micromechanics and Microengineering* 13 (6 Nov. 2003), pp. 801–808. ISSN: 0960-1317. DOI: 10.1088/0960-1317/13/6/302.

[15] Nam-Trung Nguyen and Zhigang Wu. “Micromixers-a review”. In: *Journal of Micromechanics and Microengineering* 15 (2 Feb. 2005), R1–R16. ISSN: 0960-1317. DOI: 10.1088/0960-1317/15/2/R01.

[16] Jinsong Tao, Shing Chow, and Ying Zheng. “Application of Flash Nanoprecipitation to Fabricate Poorly Water-soluble Drug Nanoparticles”. In: *Acta Pharmaceutica Sinica B* 9 (Nov. 2018). DOI: 10.1016/j.apsb.2018.11.001.

[17] Jan Kotouček et al. “Preparation of nanoliposomes by microfluidic mixing in herring-bone channel and the role of membrane fluidity in liposomes formation”. In: *Scientific Reports* 10.1 (Mar. 2020). DOI: 10.1038/s41598-020-62500-2. URL: https://doi.org/10.1038/s41598-020-62500-2.

[18] Abraham D. Stroock et al. “Chaotic Mixer for Microchannels”. In: *Science* 295 (5555 Jan. 2002), pp. 647–651. ISSN: 0036-8075. DOI: 10.1126/science.1066238.

[19] Jesús Mosquera, Isabel Garcıa, and Luis M. Liz-Marzán. “Cellular Uptake of Nanoparticles versus Small Molecules: A Matter of Size”. In: *Accounts of Chemical Research* 51.9 (Aug. 2018), pp. 2305–2313. DOI: 10.1021/acs.accounts.8b00292. URL: https://doi.org/10.1021/acs.accounts.8b00292.

[20] Bahareh Azimi et al. “Poly (lactide -co- glycolide) Fiber: An Overview”. In: *Journal of Engineered Fibers and Fabrics* 9.1 (Mar. 2014), p. 155892501400900. DOI: 10.1177/155892501400900107. URL: https://doi.org/10.1177/155892501400900107.

[21] Rajnish Sahu et al. “A nanovaccine formulation of Chlamydia recombinant MOMP encapsulated in PLGA 85:15 nanoparticles augments CD4 effector (CD44high CD62Llow) and memory (CD44high CD62Lhigh) T-cells in immunized mice”. In: *Nanomedicine: Nanotechnology, Biology and Medicine* 29 (Oct. 2020), p. 102257. DOI: 10.1016/j.nano.2020.102257. URL: https://doi.org/10.1016/j.nano.2020.102257.

[22] Vida Dennis et al. “Chlamydia trachomatis recombinant MOMP encapsulated in PLGA nanoparticles triggers primarily T helper 1 cellular and antibody immune responses in mice: a desirable candidate nanovaccine”. In: *International Journal of Nanomedicine* (May 2013), p. 2085. DOI: 10.2147/ijn.s44155. URL: https://doi.org/10.2147/ijn.s44155.

[23] Sameer Joshi et al. “Microfluidics based manufacture of liposomes simultaneously entrapping hydrophilic and lipophilic drugs”. In: *International Journal of Pharmaceutics* 514.1 (Nov. 2016), pp. 160–168. DOI: 10.1016/j.ijpharm.2016.09.027. URL: https://doi.org/10.1016/j.ijpharm.2016.09.027.

[24] Nilanjan Pal. “Studies on the Characterization, Interfacial Tension and Rheology of a Novel Polymeric Surfactant Derived from Castor Oil for Enhanced Oil Recovery”. PhD thesis. May 2015.

[25] Sameer Joshi et al. “Comprehensive Screening of Drug Encapsulation and Co-Encapsulation into Niosomes Produced Using a Microfluidic Device”. In: *Processes* 8.5 (May 2020), p. 535. DOI: 10.3390/pr8050535. URL: https://doi.org/10.3390/pr8050535.

[26] Skyla A. Duncan et al. “Prolonged Release and Functionality of Interleukin-10 Encapsulated within PLA-PEG Nanoparticles”. In: *Nanomaterials* 9.8 (July 2019), p. 1074. DOI: 10.3390/nano9081074. URL: https://doi.org/10.3390/nano9081074.